Journal of Solid State Chemistry **147,** 565–572 (1999)
Article ID jssc.1999.8419, available online at http://www.idealibrary.com on IDEAL®

Synthesis, Crystal Structure, and Magnetic Properties of FeP_3SiO_{11}: First Example of Iron(III) Silicophosphate

L. K. Elbouaanani, B. Malaman, and R. Gérardin

Laboratoire de Chimie du Solide Minéral, Université Henri Poincaré-Nancy I, associé au CNRS (UMR 7555), B.P. 239, 54506 Vandoeuvre les Nancy Cedex, France

Received March 2, 1999; in revised form May 25, 1999; accepted May 27, 1999

FeP_3SiO_{11} has been prepared by solid state reaction of $Fe(PO_3)_3$ and SiO_2 at 900°C under vacuum. This compound is isotypic with RuP_3SiO_{11} and the atomic coordinates have been refined by the Rietveld method. The unit cell is trigonal, space group *R*-3*c*, with $a = 8.2896(9)$ Å, $c = 39.054(4)$ Å, and $Z = 12$. The structure is characterized by isolated FeO_6 octahedra connected by bent P_2O_7 groups (126°) while Si_2O_7 units only share corners with P_2O_7 units. Neutron diffraction study shows that FeP_3SiO_{11} is antiferromagnetic with a Néel temperature $T_N = 3.5$ K. In this compound, the magnetic interactions arise only from Fe–O–P–O–Fe superexchange mechanism. The magnetic structure is characterized by a stacking of antiferromagnetic (001) layers of double FeO_6 octahedra sheets, with the spin perpendicular to the *c*-axis. The room temperature Mössbauer spectrum is characteristic of the Fe^{3+} valence state. The magnetic interactions are discussed.

INTRODUCTION

The Fe–P–O system presents a great number of compounds by comparison with the iron silicates (1), which are limited at normal pressure to the fayalite Fe_2SiO_4 and iscorite Fe_7SiO_{10} (2, 3). In the same way, iron(II)–$Fe_2SiP_4O_{14}$ (4) was, up to now, the only known iron silicophosphate compound.

During our investigations of the Fe–P–Si–O system, we have discovered the first example of iron III silicophosphate: FeP_3SiO_{11}. In this paper, we report on its structural and magnetic properties studied by powder X-ray diffraction, bulk magnetization, Mössbauer spectroscopy, and neutron diffraction experiments.

EXPERIMENTAL

FeP_3SiO_{11} has been obtained from the "$Fe(PO_3)_3$ + SiO_2" mixture, annealed for several days at 900°C, in a silica tube under vacuum. These starting compounds were prepared as follows:

(i) $Fe(PO_3)_3$ was prepared from a solution of $Fe(NO_3)_3$, $9H_2O$ and H_3PO_4 (in the ratio Fe:P = 1:3), which was evaporated and then annealed at 400°C under nitrogen for 24 h and finally annealed at 900°C under oxygen.

(ii) SiO_2 was obtained from silicic acid SiO_2, xH_2O annealed at 120°C to eliminate water and then annealed at 800°C for 12 h.

To know the melting point of FeP_3SiO_{11}, thermogravimetric analysis (Fig. 1) was made between room temperature and 1400°C, with a heating rate of 10°C/min up to 700°C and 1°C/min up to 1400°C. FeP_3SiO_{11} decomposes from 1050°C (~26% of loss in weight between 1050 and 1400°C) and leads to an unidentified product.

Unfortunately, all attempts to produce single crystals have failed and the crystal study has been undertaken by using powder X-ray diffraction technique. The lattice parameters were determined by a least squares fitting procedure from a Guinier pattern recorded with Si as an internal standard ($a = 5.43082$ Å). The diffracted intensities have been recorded on an INEL CPS 120 powder diffractometer (Co$K\alpha$) and the atomic positions have been refined by Rietveld profile refinements using the software FULLPROF (5).

Magnetic measurements were performed (between 4.2 and 300 K) on a MANICS magnetosusceptometer in fields up to 1.6 T.

Neutron diffraction experiments were carried out at the Institut Laue Langevin (ILL), Grenoble. The diffraction patterns were recorded with the one-dimensional curved multidetector D1b with a wavelength of 2.520 Å in the temperature range 300–1.3 K. Analysis of the patterns was performed by Rietveld profile refinements (6).

The Mössbauer data have been collected with a constant acceleration spectrometer with 1024 channels. Isomer shifts are reported with respect to α-iron at room temperature. The Mössbauer effect data were analyzed by using least-squares minimization techniques (7) to evaluate the hyperfine spectral parameters.

0022-4596/99 $30.00

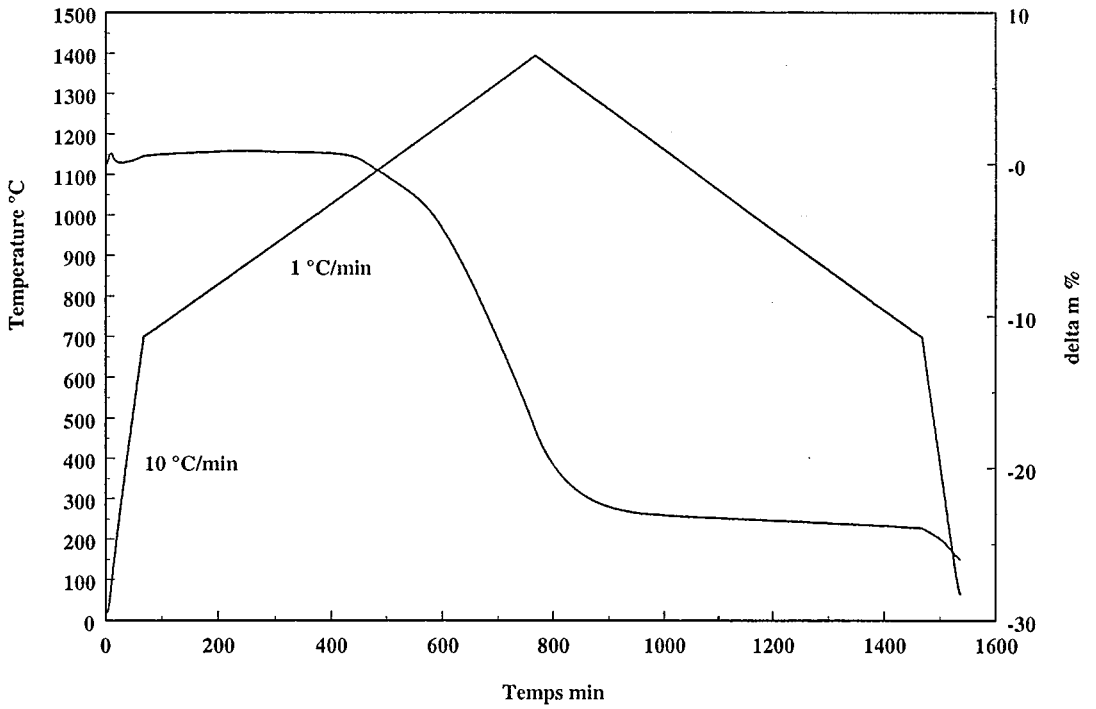

FIG. 1. Thermogravemitric analysis of FeP_3SiO_{11}.

STRUCTURE ANALYSIS

The analysis of the X-ray diffraction pattern clearly evidences that the title compound is isotypic with RuP_3SiO_{11} (8), which crystallizes in a trigonal structure (space group: R-3c, $a \sim 8.2$ Å and $c \sim 39.3$ Å, $Z = 12$).

Bearing these observations in mind, the unit cell dimensions of FeP_3SiO_{11} were refined to

$$a = 8.2896(9) \text{ Å}, \quad c = 39.054(4) \text{ Å}.$$

In a second step, using approximate atomic positions deduced from the ruthenium compound as a starting point, the final R value drops to 6%. The final atomic parameters are given in Table 1. The observed and calculated diffraction profiles are shown in Fig. 2. (Some extremely weak reflections remained unindexed during the refinements; they probably originate from an impurity.)

Description

The crystal structure of FeP_3SiO_{11} is a three-dimensional nework of corner-sharing FeO_6, P_2O_7, and Si_2O_7 units. The six terminal oxygens of Si_2O_7 are bonded to six surrounding P_2O_7 subunits. The "Si_2O_7–$6P_2O_7$" silicophosphate ions are connected via FeO_6 octahedra.

TABLE 1
Atomic Parameters for FeP_3SiO_{11} at 295 K Using X-Ray Diffraction Data and at 5 K Using Neutron Diffraction Study

		X-ray diffraction $a = 8.2896(9)$ Å, $c = 39.054(4)$ Å $R_{Bragg} = 6\%$			Neutron diffraction $a = 8.265(1)$ Å, $c = 38.976(8)$ Å $R_{Bragg} = 2.4\%$		
Atom	Site	x	y	z	x	y	z
Fe	12(c)	0	0	0.1572(2)	0	0	0.1576(8)
P	36(f)	0.3729(7)	0.0379(7)	0.1192(1)	0.374(5)	0.042(4)	0.1204(8)
Si	12(c)	0	0	0.0406(2)	0	0	0.041(1)
O1	36(f)	0.046(1)	0.200(1)	0.0546(3)	0.043(3)	0.204(3)	0.0535(7)
O2	36(f)	0.226(2)	0.074(1)	0.1267(2)	0.219(5)	0.078(4)	0.1280(7)
O3	36(f)	0.139(1)	0.227(1)	0.1912(2)	0.133(4)	0.225(3)	0.1881(7)
O4	18(c)	0.209(2)	0	0.75	0.208(4)	0	0.75
O5	6(b)	0	0	0	0	0	0

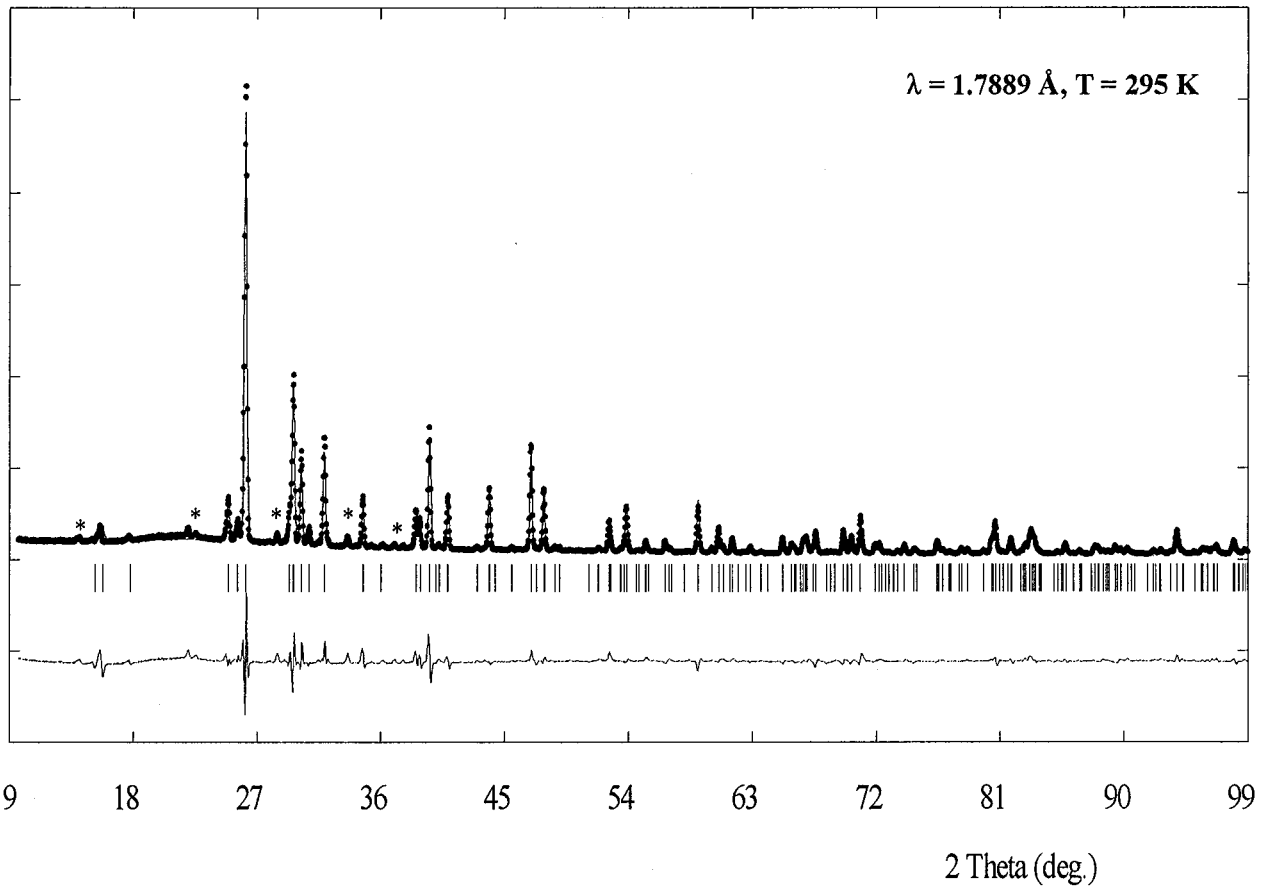

FIG. 2. Observed and calculated X-ray powder diffraction profile of FeP_3SiO_{11} at 295 K (*, impurities).

The topology of the silicate anion may be described as "unbranched" oligosilicate, following the terminology of Liebau (9), and written as $\{uB,2t\}[Si_2O_7]^{6-}$. Figure 3a illustrates the projection of the structure on the (0 0 1) plane.

The bond lengths and angles are given in Table 2. For Si_2O_7, $Si–O_{terminal} = 1.600(9)$ Å, $Si–O_{bridge} = 1.586(8)$ Å, and angle $Si–O–Si = 180°$. The P–O bond lengths are 1.60(1) Å (with O atoms connected with Si atoms), 1.570(8) Å (with a bridging O atom) and ~1.43(2) Å (with O atoms connected with Fe atoms), yielding an average value of 1.53 Å, in agreement with to the classical value of 1.536 Å value given by Corbridge (10). The PO_4 tetrahedra are smaller than the SiO_4 tetrahedra as currently observed in silicophosphates. The P–O–P links are bent and the angle of ~126° is near the smallest value observed in other diphosphates (11). A similar value is observed for RuP_3SiO_{11}. The P_2O_7 conformations are of oblique form.

Iron atoms are on threefold axes and embedded in isolated FeO_6 octahedra made of two kind of oxygen atoms (O_2 and O_3, Table 2). The Fe–O interatomic distances are 2.04(1) Å and 2.11(1) Å yielding an almost regular octahedron. As still measured in RuP_3SiO_{11}, the P–O bond of the Fe–O_3–P–O_2–Fe pathway is short, whereas the corresponding O_3–P–O_2 angle is relatively large (~119°).

As shown on Fig. 3b, this structure can also be described as constructed from identical layers. Each layer is made of FeO_6 and Si_2O_7 units connected through PO_4 subunits (see Fig. 3). The layers are stacked along the *c*-axis sharing the apices of the PO_4 tetrahedra of the P_2O_7 units.

In a layer, the iron atoms build double-plane Kagomé nets (Fig. 3). The Fe–Fe interaction from one plane to the other is assumed by Fe–O–P–O–Fe superechange, whereas a Fe–O–P–O–P–O–Fe super-superexchange occurs between the layers. This description will be useful during the analysis of the magnetic structure.

MAGNATIC MEASUREMENTS

Between 4.2 and 300 K, FeP_3SiO_{11} is paramagnetic and the temperature dependence of its inverse susceptibilty obeys the Curie–Weiss law with the apparent Curie molar constant $C_M = 4.6$ and $\theta_P = -5.9$ K. The effective magnetic moment value $\mu = 6.08\ \mu_B$ is close to the 5.92 μ_B value expected for a high-spin iron III compound. The

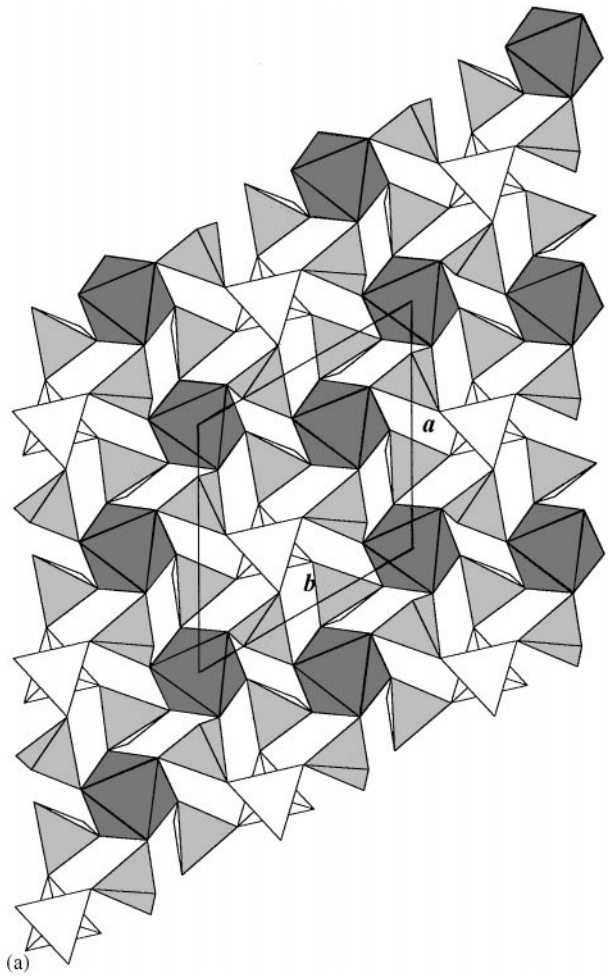

FIG. 3. (a) Projection on the *ab* plane of the FeP_3SiO_{11} structure. Only one independent layer is represented (see (*b*)). Dark polyhedra are FeO_6 and open polyhedra are Si_2O_7. Shaded tetrahedra are PO_4 units. (b) The unit cell projected on the (1 1 0) plane, showing six identical layers

measurement of the magnetization versus field at 4.2 and 300 K does not detect any spontaneous magnetism.

MÖSSBAUER STUDY

The room temperature spectrum has been fitted by a least-squares method with one Lorentz-type quadrupole doublet. The quadrupole splitting has a value of 0.16 mm/s, in agreement with the almost regular oxygen environment of the ion.

The isomer shift of 0.45 mm/s is characteristic of a high-spin Fe^{3+} in an octahedral crystal field (12). The most striking feature is the high value of this parameter; let us recall that the usual range in oxides is, according to MENIL (12), 0.29–0.50 mm/s for Fe^{3+} in VI coordination. The high value observed in FeP_3SiO_{11} is not unexpected, as it has been well established (1) that, thanks to the inductive effect, the Fe–O bond in phosphates is rather highly ionic, and this is especially true in diphosphates.

A 4.2 K spectrum does not exhibit any new features; it confirms that the magnetic order onset takes place below this temperature (see below).

NEUTRON DIFFRACTION STUDY

Magnetic Structure

Neutron diffraction patterns recorded at 5 and 1.3 K are shown in Fig. 4. At 5 K, the pattern is characteristic of the only nuclear scattering. The extinction rules of the space group *R*-3*c* are fullfilled and confirm unambiguously the crystal structure deduced from the room temperature X-ray study. The refined nuclear parameters together with the residual factors are gathered in Table 1. The main distances are given in Table 2.

Below 4 K, the diffraction pattern reveals an increase of the intensities of some nuclear reflections, which indicates the occurrence of a magnetic ordering of the Fe sublattice. Few magnetic contributions are observed (see Fig. 4).

As shown in the previous section, the FeP_3SiO_{11} structure may be described as made of layers stacked along the *c*-axis within which the iron atoms build (001) double-plane Kagomé nets. The best fit to the data corresponds to ferromagnetic (001) Fe planes, antiferromagnetically coupled in each layer, with the moment perpendicular to the *c*-axis. The magnetic structure is illustrated on Fig. 5.

At 1.3 K, the refined moment value is $\mu_{Fe^{3+}} = 4.44(8)\ \mu_B$ ($R_{Nuc} = 1.8\%$ and $R_{Mag} = 3.9\%$), a value expected for a high-spin iron III. The thermal variation of the magnetic moment (Fig. 6) yields a Néel temperature of 3.5(5) K. The observed and calculated intensities are given in Table 3.

DISCUSSION

The most striking feature of the FeP_3SiO_{11} magnetic structure is the absence of neither direct "cation–cation" nor "cation–anion–cation" interactions. On the whole, it appears that only long-range superexchange occurs in this compound. Actually, the magnitude of the Fe–O–P–O–Fe interaction is an open question, as Néel temperatures of 29 and 47 K have been reported in $NaFeP_2O_7$ (13) and $Na_3Fe_2(PO_4)_3$ (14), respectively, and only 4 K in $KBaFe_2(PO_4)_3$ (15). Moreover, here we have both Fe–O–P–O–Fe and Fe–O–P–O–P–O–Fe interactions and it is clear that we have to consider two types of interactions, intra- and interlayers, from the strongest to the weakest.

In each layer, FeO_6 polyhedra are connected only by Fe–O–P–O–Fe bonds. As shown on Fig. 5, in the iron double-plane net, iron atoms of one plane are linked to three iron atoms of the other plane through three double Fe–O–P–O–Fe pathways. This long-range superexchange Fe–O–P–O–Fe is characterized by the angle on phosphorus

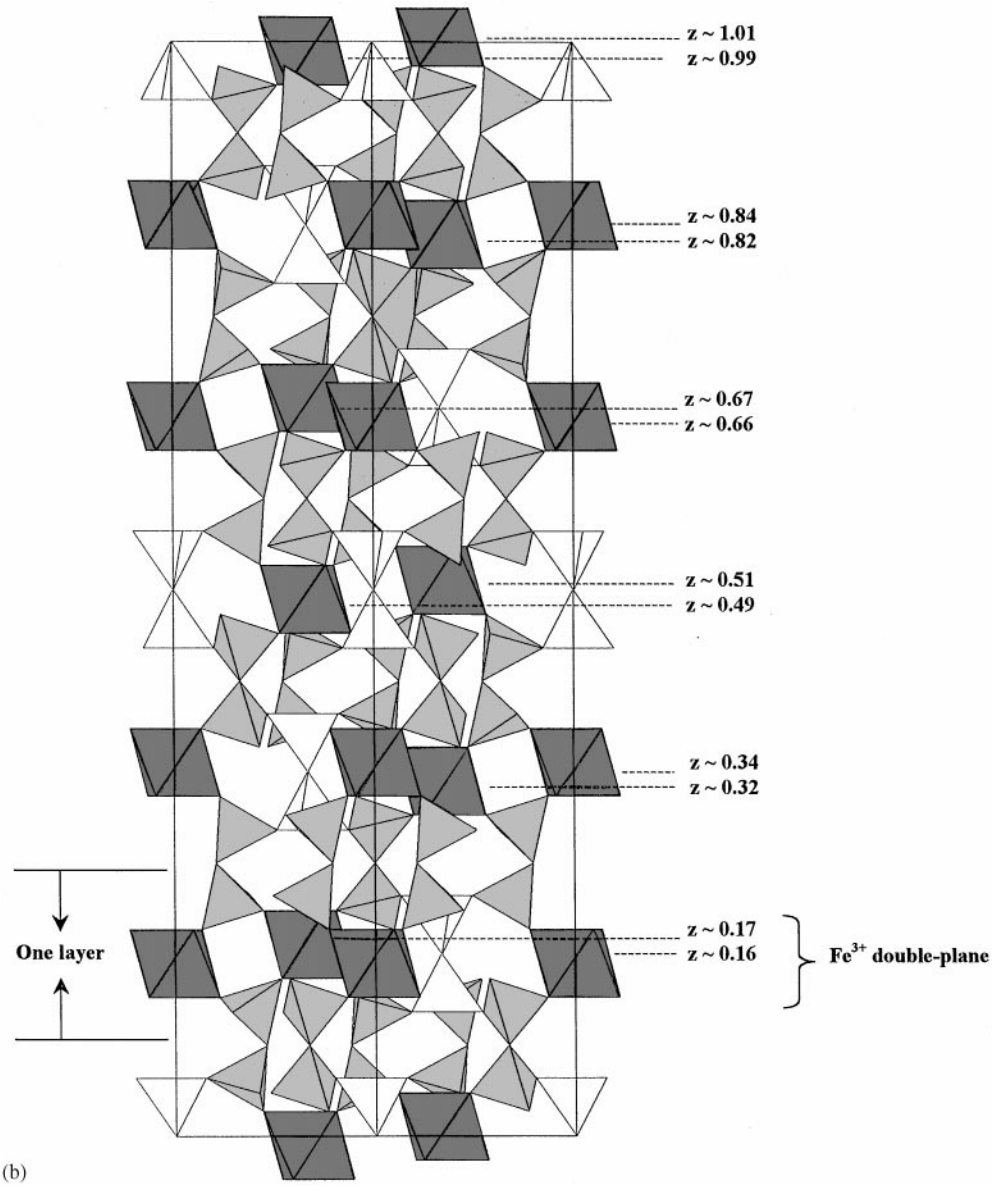

FIGURE 3—*Continued*

(119°) and by the sum of the two Fe–O bonds (4.15 Å) and the two P–O bonds which are surprisingly short in this structure (1.48 Å). As regards its strength, this superexchange is more effective the shorter the exchange pathway and the closer the angle at the phosphorus atom to the tetrahedral angle (15). The angles around phosphorus are greater than 109°, due to the existence of P–O–P bonds, and this weakens the interactions (16).

As shown in Fig. 5a, each iron of one layer is antiferromagnetically coupled with one iron of the adjacent layer through three Fe–O–P–O–P–O–Fe pathways. These interlayer interactions are probably still weaker than the intralayers ones as they call in super-super exchange actions.

If we consider, in a first approximation, that the intralayer interactions determine the long-range order, and calling J this interaction;

$$T_N = -2JS(S+1)n/3k = 4K,$$

Where $S = 2.5$ and n is the number of such interactions ($n = 3$); hence,

$$J = -2 \times 10^{-2}\ \text{meV} = -0.16\ \text{cm}^{-1},$$

which is weak compared with $J = -0.37\ \text{cm}^{-1}$ ($T_N = 29$ K) in $NaFeP_2O_7$ (13) and $-0.36\ \text{cm}^{-1}$ ($T_N = 18$ K) in $Fe_3(P_2O_7)_2$ (17).

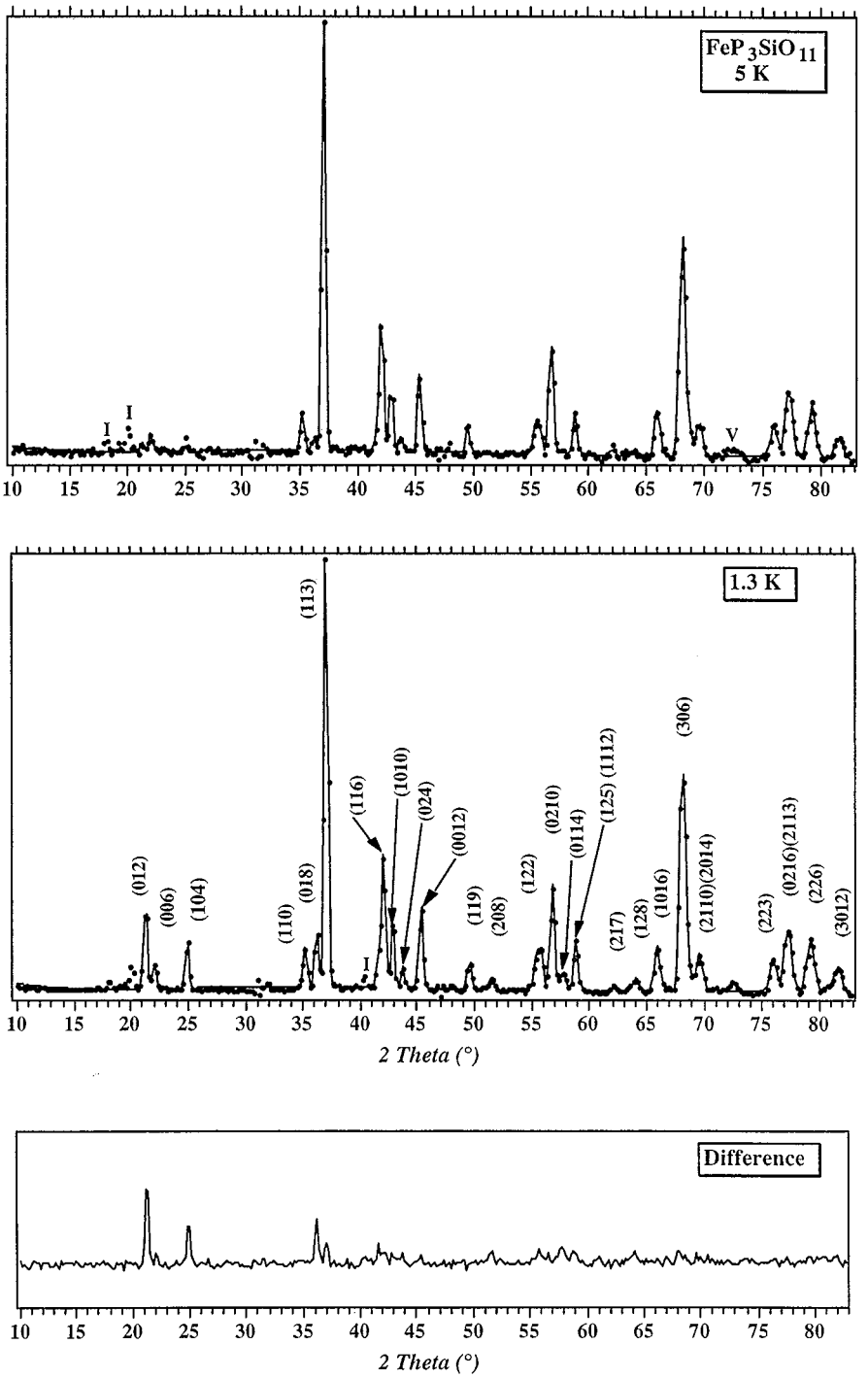

FIG. 4. Observed and calculated neutron powder diffraction profiles of FeP_3SiO_{11} at 5 and 1.3 K and difference between them. (I, Impurities; V, vanadium sample holder).

CONCLUSION

FeP_3SiO_{11} is the first example of an iron(III)silicophosphate. Isotypic with RuP_3SiO_{11}, its structure is characterized by a stacking of double sheet of isolated FeO_6 octahedra connected by bent P_2O_7 groups, while Si_2O_7 units only share corners with P_2O_7 units. Neutron diffraction study shows that FeP_3SiO_{11} orders antiferromagnetically

TABLE 2
Main Interatomic Distances (Å) and Angles (°), at 295 K from X-Ray Powder Study and at 5 K from Neutron Diffraction Study

		X-Ray diffraction	Neutron diffraction
Fe–O2	(×3)	2.04(1)	1.96(4)
Fe–O3	(×3)	2.113(9)	2.01(3)
P–O2		1.42(2)	1.48(6)
P–O3		1.429(9)	1.50(5)
P–O4		1.570 (8)	1.60(3)
P–O1		1.60(1)	1.57(4)
O2–P–O3		118.7(6)	119(3)
O2–P–O4		108.8(5)	109(3)
O2–P–O1		109.2(4)	109(2)
O3–P–O4		105.6(6)	108(2)
O3–P–O1		111.2(6)	110(3)
O4–P–O1		101.8(6)	100(2)
P–O4–P		126(1)	129(3)
Si–O5		1.586(8)	1.60(4)
Si–O1	(×3)	1.600(9)	1.61(3)
O5–Si–O1	(×3)	110.0(5)	108(2)
O1–Si–O1	(×3)	109.0(5)	111(2)
Si–O5–Si		180	180

below $T_N = 3.8$ K. In this compound, the magnetic interactions arise from antiferromagnetic Fe–O–P–O–Fe and Fe–O–P–O–P–O–Fe superexchange mechanisms only.

TABLE 3
Observed and Calculated Intensities at 1.3 K of FeP_3SiO_{11}

h k l	2 Theta (°)	I_{Nuc}	I_{Mag}	I_{Tot}	I_{Obs}
0 1 2	21.62	679	5753	6,432	6,527
0 0 6	22.37	1,297	561	1,858	1,915
1 0 4	25.24	394	2895	3,289	3,614
1 1 0	35.51	2,715	0	2,715	2,927
0 1 8	36.47	644	3201	3,845	3,869
1 1 3	37.32	30,110	0	30,110	30,305
2 0 2	41.95	1,518	1208	2,726	2,725
1 1 6	42.37	9,747	479	10,226	10,211
1 0 10	43.20	4,973	316	5,289	5,240
0 2 4	44.06	973	675	1,648	1,621
0 0 12	45.66	6,200	380	6,580	6,628
1 1 9	49.86	2,234	0	2,234	2,130
2 0 8	51.81	2.	1100	1,102	1,214
2 1 1	55.67	2,608	0	2,608	2,784
1 2 2	56.10	2,613	1158	3,771	3,620
0 2 10	57.11	9,761	129	9,890	9,936
2 1 4	57.82	19	654	673	678
0 1 14	58.12	519	308	827	853
1 2 5	59.08	153	0	153	155
1 1 12	59.14	3,817	960	4,777	4,806
2 1 7	62.38	464	0	464	440
1 2 8	64.4	377	1145	1,522	1,594
1 0 16	66.25	5,173	0	5,173	5,123
3 0 6	68.48	25,259	132	25,391	25,617
2 1 10	69.08	2,010	142	2,152	2,045
1 1 15	69.90	3,548	0	3,548	3,405
2 0 14	69.99	478	508	986	973
2 2 3	76.27	4,100	0	4,100	4,130
0 2 16	77.48	5,013	0	5,013	4,964
2 1 13	77.72	4,398	0	4,398	4,311
2 2 6	79.58	7,226	86	7,312	7,144
3 0 12	81.89	2,679	335	3,014	3,077

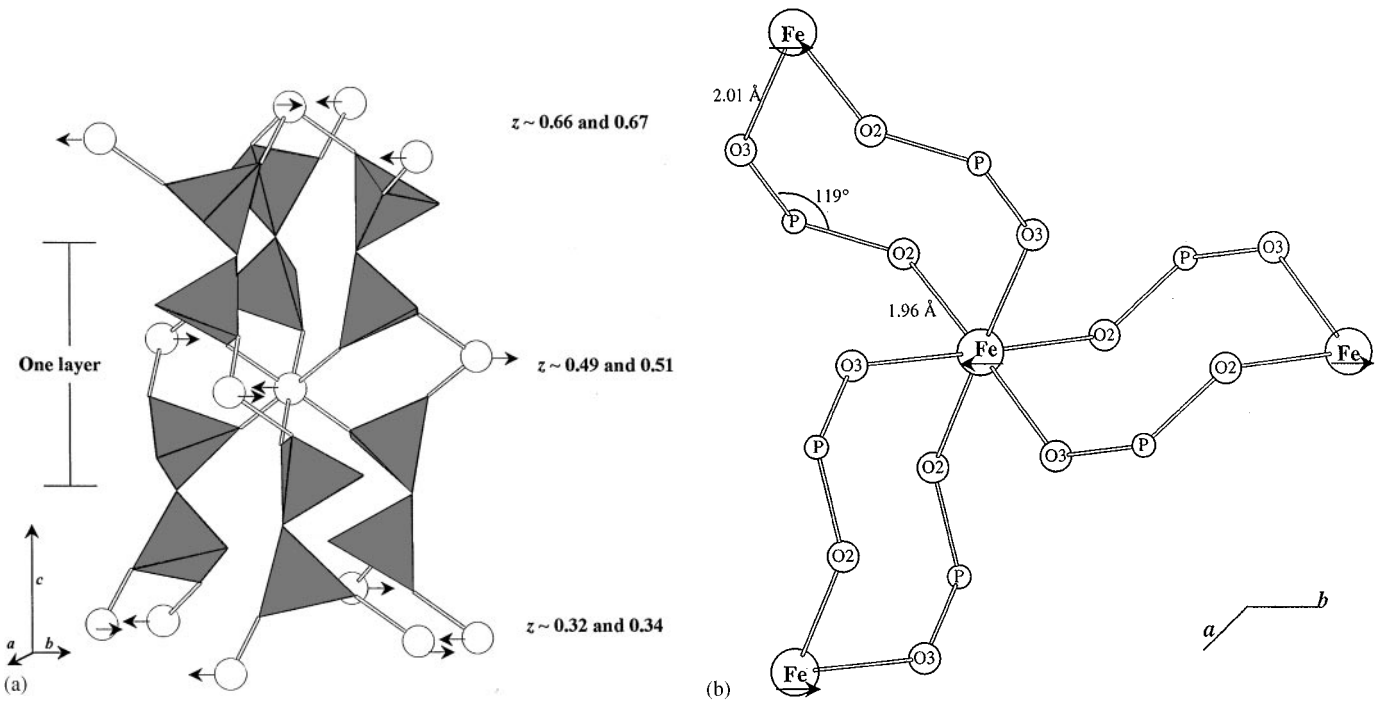

FIG. 5. (a) Magnetic structure of FeP_3SiO_{11}. Open circles are Fe atoms; shaded tetrahedra are P_2O_7 units. Two types of interactions: Interactions intralayer between Fe atom ($z \sim 0.49$) and its three neighbors ($z \sim 0.51$) (see (b)). Interactions interlayer with the two adjacent layers ($z \sim 0.32$, 0.34 and $z \sim 0.66$, 0.67) through the P_2O_7 units. (b) Projection of one layer showing the intralayer superexchange pathway: each iron is antiferromagnetically coupled to three irons neighbors through three double Fe–O–P–O–Fe paths.

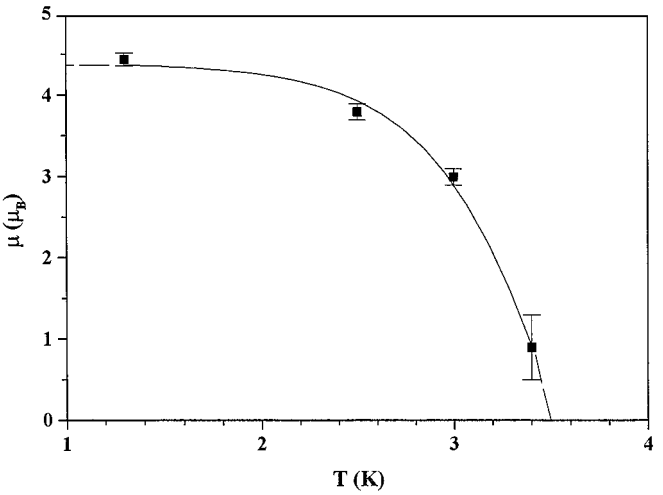

FIG. 6. Thermal dependence of the Fe^{3+} magnetic moment in FeP_3SiO_{11}.

REFERENCES

1. C. Gleitzer, *Eur. J. Solid Inorg. Chem.* **28,** 77 (1991).
2. J. Smuts, J. Steyn, and J. Boeyens, *Acta Crystallogr. Sect. B* **25,** 1251 (1969).
3. A. Modaressi, B. Malaman, C. Gleitzer, and R. Tilley, *J. Solid State Chem.* **60,** 107 (1985).
4. R. Glaum and A. Schmidt, *Acta Crystallogr. Sect. C* **52,** 762 (1996).
5. J. Rodriguez-Carvajal, FULLPROF Program, Laboratoire Leon Brillouin, 1998.
6. H. M. Rietveld, *J. Appl. Crystallogr.* **2,** 65 (1969).
7. G. Le Caer, private communication.
8. H. Fukuoka, H. Imoto, and T. Saito, *J. Solid State Chem.* **121,** 247 (1996).
9. F. Liebau, "Structural Chemistry of Silicates." Springer-Verlag, Berlin, 1985.
10. D. Corbridge, *Bull. Soc. Fr. Mineral. Cristallogr.* **94,** 271 (1971).
11. A. G. Nord and P. Kierkegard, *Chem. Scr.* **15,** 27 (1980).
12. F. Menil, *J. Phys. Chem. Solids* **46,** 763 (1985).
13. L. Terminiello and R. C. Mercader, *Hyperfine Interact.* **50,** 651 (1989).
14. D. Beltran-Porter, R. Olazcuaga, L. Fournes, F. Menil, and G. Le Flem, *Rev. Phys. Appl.* **15,** 1155 (1980).
15. P. D. Battle, A. K. Cheetham, W. T. A. Harrison, and G. J. Long, *J. Solid State Chem.* **62,** 16 (1986).
16. P. W. Anderson, *in* "Magnetism" (G. Rado and H. Shul, Eds.), Vol. 1, p. 25. Academic Press, New York, 1963.
17. G. Venturini, M. Ijjaali, B. Malaman, and C. Gleitzer, *Eur. J. Solid State Inorg. Chem.* **29,** 1189 (1992).